Technical Notes

TECHNICAL NOTES are short manuscripts describing new developments or important results of a preliminary nature. These Notes cannot exceed 6 manuscript pages and 3 figures; a page of text may be substituted for a figure and vice versa. After informal review by the editors, they may be published within a few months of the date of receipt. Style requirements are the same as for regular contributions (see inside back cover).

Stagnation Streamline Turbulence

Dale B. Taulbee* and Le Tran†
University of New York at Buffalo, Buffalo, New York

TURBULENCE in the far-field flow approaching a stagnation point tends to decay by dissipation and grow by production due to mean field gradients. Near the surface where the mean flow gradients are steepest, diffusional transport also becomes important. The resulting boundary layer on the surface near the stagnation point may be considered to be pseudoturbulent or disturbed laminar, and the surface friction and heat transfer can be significantly different than the stagnation flow with no turbulence.

Although there have been many analyses of the stagnation flow process with turbulence, only Refs. 1-5 have considered the entire stagnation streamline process. Traci and Wilcox[1] and Sunden[2] use the k-ω two-equation model where ω is the pseudovorticity. Although the kinetic energy distributions on the stagnation streamline and heat transfer at the stagnation point predicted by Refs. 1 and 2 agree with each other, Sunden[2] had to use low Reynolds number formulations of the model parameters to obtain agreement with experiment. Strahle et al.[4] used the k-ϵ model of Lam and Bremhorst[6] to solve for the inner solutions with the boundary conditions found in Ref. 3, where the outer solution was obtained. They had to adjust a parameter in the solution for the outer flow to get agreement with experiment. Hijikata et al.[5] recognized the shortcomings of the k-ϵ model when applied to the stagnation flow and developed a three-equation model, the third equation in addition to those for k and ϵ being written for the anisotropy between the streamwise and transverse Reynolds stress components. They had to modify the return-to-isotropy expression in that equation to obtain agreement with experimental data.

Two equation models of turbulence use the constitutive relation

$$-\overline{u_i u_j} = \nu_t\left(\frac{\partial U_i}{\partial x_j} + \frac{\partial U_j}{\partial x_i}\right) - (2/3)k\delta_{ij} \tag{1}$$

for the Reynolds stresses. This equation works well for the shear components; however, it is not accurate for the normal components. The example of a homogeneous shear flow where $U = U(y)$ and Eq. (1) gives $\overline{u^2} = \overline{v^2} = \overline{w^2} = 2k/3$ shows that it is not consistent with experimental observations, even though $\overline{uv} = -\nu_t\, dU/dy$ is satisfied. Furthermore, Eq. (1) shows that if the flow has no mean flow gradients, the turbulence can only be isotropic, which may not be true. If the flow is shear dominated, then turbulent models using Eq. (1) work well. However, if the shear is zero or weak and the production of turbulence is governed by normal stresses as in the present problem, then the model prediction may be inaccurate. To avoid these difficulties, the dynamic equations for the Reynolds stresses should be used. Comparisons between predictions from the k-ϵ model and the Reynolds stress model will be presented to illustrate the inadequacy of the k-ϵ model with Eq. (1) for stagnation flow.

The stagnation point boundary layer, where the flow is directly affected by the wall and viscous effects are important, has a thickness estimated by

$$\delta/R \cong 0.54(Tu\,\ell_\infty/R)^{1/2}$$

where Tu is the intensity, ℓ_∞ is the length scale of the far-upstream turbulence, and R is the radius of the cylinder. This relation was obtained from $\delta/R \cong 2.4/Re^{1/2}$ for the laminar stagnation boundary layer on a circular cylinder, but using a turbulent eddy viscosity $\nu_t = c_\mu k^{1/2}\ell$, with $c_\mu = 0.09$ in place of the laminar viscosity and assuming that the turbulence intensity and length scales do not change in the outer flow. This relation shows that the boundary-layer thickness in the stagnation region can be on the order of 0.01-0.1 of the leading-edge radius, depending on the magnitude of Tu and ℓ_∞.

In the flow outside the boundary layer, an order-of-magnitude analysis of the momentum equation shows that the turbulence does not significantly affect the mean flow. The turbulent stresses are negligible, and the mean flow is essentially inviscid and given by the potential flow solution

$$U = U_\infty(1 - R^2/x^2) \tag{2}$$

along the stagnation streamline for a circular cylinder where U_∞ is far freestream uniform flow velocity and x is measured from the center of the cylinder. Bearman[7] measured the velocity along the stagnation streamline for flow over a blunted symmetrical airfoil shape with freestream turbulence and found the data to agree very well with the potential flow velocity until a location relatively near the surface.

Using similar arguments, the diffusive transport terms in the turbulent kinetic energy equation can be neglected. The energy equation then can be written along the stagnation streamline as

$$U\frac{dk}{dx} = -(\overline{u^2} - \overline{v^2})\frac{dU}{dx} - \epsilon \tag{3}$$

where $k = \overline{q^2}/2$ is the turbulent kinetic energy, ϵ is the dissipation, $\overline{u^2}$ is the streamwise Reynolds stress component, $\overline{v^2}$ is the lateral component, and the production $P = -\overline{u^2}\,\partial U/\partial x - \overline{v^2}\,\partial V/\partial y$ was simplified with the continuity equation $\partial U/\partial x + \partial V/\partial y = 0$ for incompressible flow. The model equation for the dissipation, again neglecting diffusive transport, is

$$U\frac{d\epsilon}{dx} = \frac{\epsilon}{k}(C_{\epsilon_1}P - C_{\epsilon_2}\epsilon) \tag{4}$$

where, for the standard k-ϵ model, $C_{\epsilon_2} = 1.92$ and $C_{\epsilon_1} = 1.44$, as given by Launder et al.[8]

In the k-ϵ model, the Reynolds stresses are obtained from Eq. (1), and the production term in Eq. (3) is evaluated as

$$P = -(\overline{u^2} - \overline{v^2})\frac{\partial U}{\partial x} = 2\nu_t\left(\frac{\partial U}{\partial x} - \frac{\partial V}{\partial y}\right)\frac{\partial U}{\partial x} = 4\nu_t\left(\frac{\partial U}{\partial x}\right)^2 \tag{5}$$

where $\nu_t = C_\mu k^2/\epsilon$ and $C_\mu = 0.09$ as given in Ref. 8. In the outer flow, the velocity gradient $\partial u/\partial x$ can be obtained from Eq. (2). Equations (3) and (4) can be integrated as initial-valued ordinary differential equations from the far freestream to a point outside the boundary layer. The far freestream values are

Received Nov. 16, 1987; revision received Feb. 4, 1988.

*Professor, Department of Mechanical and Aerospace Engineering.
†Research Assistant, Department of Mechanical and Aerospace Engineering.

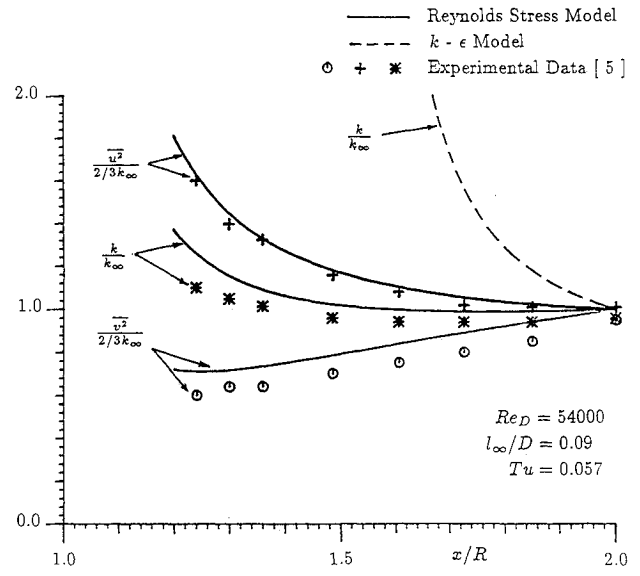

Fig. 1 Comparison of turbulent kinetic energy on the stagnation streamline for small freestream turbulence length scale.

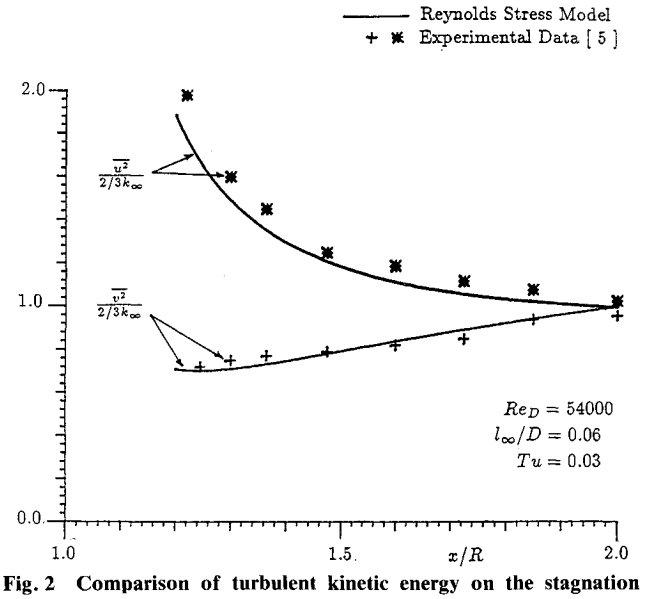

Fig. 2 Comparison of turbulent kinetic energy on the stagnation streamline for small freestream turbulence length scale.

$k_\infty = 1.5(TuU_\infty)^2$ and $\epsilon_\infty = k_\infty^{3/2}/\ell_\infty$, where the turbulent intensity Tu and the length scale ℓ_∞ are specified. Solutions were found numerically corresponding to the experimental conditions of Hijikata.[5] As seen in Fig. 1, the k-ϵ model gives unrealistically large kinetic energies as the flow approaches the surface. The component energies (not shown) are also very poor when compared to the experimental data for the cases shown in Figs. 1 and 2.

The anisotropy in the Reynolds stresses that govern the production term in Eq. (3) arises from the rapid part of the pressure-strain correlation $\overline{p(\partial u_i/\partial x_j + \partial u_j/\partial x_i)}$, which accounts for the distortion of the turbulence by the mean flow. The turbulent-turbulent interaction part of the pressure-strain correlation tends to return the turbulence to isotropy. In the k-ϵ model, the normal stresses are modeled with a gradient hypothesis [Eq. (1)] that does not properly reflect the nature of the pressure-strain processes.

In order to accurately determine the normal Reynolds stress components, they should be determined from a Reynolds stress turbulence model. The dynamic equations for $\overline{u^2}$ and $\overline{v^2}$ along the stagnation streamline are

$$U\frac{d\overline{u^2}}{\partial x} = -2\overline{u^2}\frac{\partial U}{\partial x} + 2\overline{\frac{p}{\rho}\frac{\partial u}{\partial x}} - (2/3)\epsilon \tag{6}$$

$$U\frac{d\overline{v^2}}{dx} = -2\overline{v^2}\frac{\partial V}{\partial y} + 2\overline{\frac{p}{\rho}\frac{\partial v}{\partial y}} - (2/3)\epsilon \tag{7}$$

where, as before, the diffusive transport terms have been neglected for the outer flow. The particular Reynolds stress model used is given by Lumley,[9] where for this problem

$$2\overline{\frac{p}{\rho}\frac{\partial u}{\partial x}} = -8C\,\overline{u^2}\frac{\partial U}{\partial x} + 4C\,\overline{v^2}\frac{\partial V}{\partial y} + 4(C + 1/10)\overline{q^2}\frac{\partial U}{\partial x} + C_1\epsilon(\overline{u^2}/\overline{q^2} - 1/3) \tag{8}$$

$$2\overline{\frac{p}{\rho}\frac{\partial v}{\partial y}} = +4C\,\overline{u^2}\frac{\partial U}{\partial x} - 8C\,\overline{v^2}\frac{\partial V}{\partial y} + 4(C + 1/10)\overline{q^2}\frac{\partial V}{\partial y} + C_1\epsilon(\overline{v^2}/\overline{q^2} - 1/3) \tag{9}$$

where $C = -0.16$ and

$$C_1 = 2 + \exp(-7.77/\sqrt{Re_t})\,F/9\,\{72/\sqrt{Re_t} + 80.1\,\ell n[1 + 62.4(-II + 2.3III)]\} \tag{10}$$

where $II = -b_{ij}b_{ji}/2$ and $III = b_{ij}b_{jk}b_{ki}/3$ are invariants of the anisotropic tensor $b_{ij} = \overline{u_iu_j}/q^2 - \delta_{ij}/3$ and the turbulent Reynolds number is $Re_t = \overline{q^2}^2/9\nu\epsilon$. Also, the parameters in the dissipation equation, Eq. (4), are in Lumley's notation

$$2C_{\epsilon_1} = \psi_1 = 2.4, \qquad 2C_{\epsilon_2} = \psi_0$$

where

$$\psi_0 = 14/5 + 0.98[\exp(-2.83/\sqrt{Re_t})]\,[1 - 0.33\,\ell n(1 - 55II)] \tag{11}$$

Equations (3), (4), (6), and (7) can be solved to determine the variation of u^2, v^2, k, and ϵ along the stagnation streamline in the outer flow starting from values $u_\infty^2 = v_\infty^2 = 2k_\infty/3$, where $k_\infty = 1.5(TuU_\infty)^2$ and $\epsilon_\infty = k_\infty^{3/2}/\ell_\infty$.

The results from the Reynolds stress model are shown in Figs. 1 and 2 for the experiment performed by Hijikata.[5] It is seen that the Reynolds stress model results are in good agreement with the data. Some of the differences between the predictions and experiment can be attributed to the apparent anisotropy in the data, which can be seen at the location $x/R = 2$ in Figs. 1 and 2. The calculation was initiated upstream of the first data point at $x/R = 5$, and significant differences in the components did not occur until after $x/R = 2$. Better predictions can be obtained if the calculations are initiated at $x/R = 2$ with the experimental values for the components. In comparing Figs. 1 and 2, it is seen that there is very little difference in the predictions for the two cases, although the experiments show somewhat greater differences when the turbulent intensity and length scale are changed.

In the experiment of Hijikata,[5] the length scales of the far freestream turbulence are much smaller than the cylinder radius. Shown in Fig. 3 are the Reynolds stress model predictions for the experiments of Britter et al.,[10] where the turbulent length scales are on the order of or larger than the cylinder radius. The comparison with the data is poor, and the k-ϵ model predictions (not shown) are poorer. The reason that the predictions are poor for this case is that single-point closure models really do not apply to the situation where the length scale ℓ_∞ is on the order of or larger than the cylinder radius. For this situation, turbulence eddies approaching the cylinder do not see a uniform strain field. Different parts of the same eddy are affected by different strain rates since they are much larger than the local length scale of the mean flow velocity gradient. Single-point closure models are based on the

$Re_D = 27400$	Reynolds Stress Model	Data [10]
$l_\infty/D = 1.43, Tu = 0.057$	A	+
$l_\infty/D = 0.78, Tu = 0.045$	B	*
$l_\infty/D = 0.35, Tu = 0.046$	C	⊙

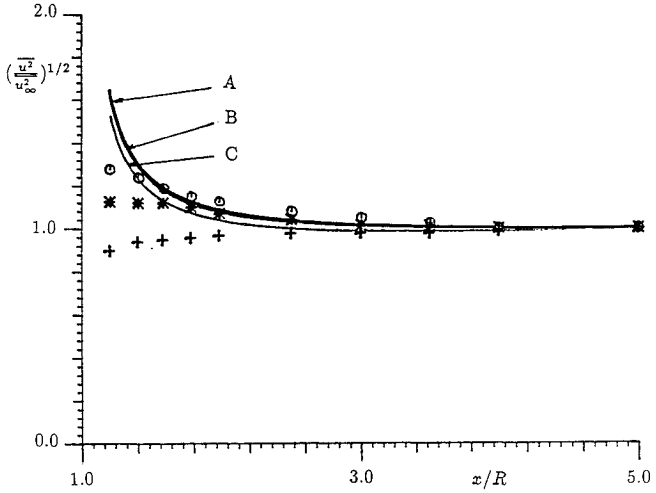

Fig. 3 Comparison of turbulent kinetic energy on the stagnation streamline for large freestream turbulence length scale.

assumption that the flow is locally homogeneous, which is not the case when the length scale is on the order of or larger than the body dimension.

In order to define the entire stagnation streamline process, an inner (boundary-layer) set of equations for the mean velocity and Reynolds stresses needs to be solved and matched to the outer flow solution in a manner similar to that done by Strahle et al.[4] for the k-ϵ model. Alternatively, the entire streamline flow from the surface to the far freestream could be directly solved with equations that contain diffusional-transport terms, which are important near the surface. This method was used by Hijikata et al.[5] with their three-equation model. Profiles for the mean velocity, kinetic energy, etc., obtained from the inner part of the stagnation streamline solution could then be used as initial conditions for a boundary-layer calculation on the surface away from the stagnation point. Taulbee et al.[11] used the near-surface profiles from the stagnation streamline solution to initiate a k-ϵ model boundary-layer calculation to obtain heat-transfer distributions on gas turbine blades.

In summary, it is stated that the two-equation turbulence model, which uses a gradient hypothesis for the Reynolds stresses, is not applicable for determining turbulence in stagnating flow. The Reynolds stress model of Lumley[9] gives good results when the length scale is small compared to the body dimension. Single-point closure models are not applicable when the length scale is as large or larger than the body dimension.

References

[1]Traci, R. M. and Wilcox, D. C., "Freestream Turbulence Effects on Stagnation Point Beat Transfer," *AIAA Journal,* Vol. 13, July 1975, pp. 890–896.

[2]Sunden, B., "A Theoretical Investigation of the Effect of Freestream Turbulence on Skin Friction and Heat Transfer for a Bluff Body," *International Journal of Heat Mass Transfer*, Vol. 22, July 1979, pp. 1125–1135.

[3]Strahle, W. C., "Stagnation Point Flow with Freestream Turbulence—The Matching Conditions," *AIAA Journal,* Vol. 23, Nov. 1985, pp. 1822–1824.

[4]Strahle, W. C., Sigman, R. K., and Meyer, W. L., "Stagnating Turbulent Flows," *AIAA Journal,* Vol. 25, Aug. 1987, pp. 1071–1077.

[5]Hijikata, K., Yoshida, H., and Mori, Y., "Theoretical and Experimental Study of Turbulence Effects on Heat Transfer Around the Stagnation Point of a Cylinder," *Proceedings of the 7th International Conference,* Vol. 3, Hemisphere, Washington, DC, 1982, pp. 165–170.

[6]Lam, C. K. G. and Bremhorst, K. A., "Modified Form of the k-ϵ Model for Predicting Wall Turbulence," *Journal of Fluids Engineering,* Vol. 103, No. 3, Sept. 1981, pp. 456–460.

[7]Bearman, P. W., "Some Measurements of the Distortion of the Turbulence Approaching a Two-Dimensional Bluff Body," *Journal of Fluid Mechanics,* Vol. 53, Pt. 3, June 1972, pp. 451–467.

[8]Launder, B. E., Morse, A. P., Rodi, W., and Spaulding, D. B., "The Prediction of Free-Shear Flows—A Comparison of the Performance of Six Turbulence Models," *Proceedings of the Langley Free-Shear Flows Conference,* Vol. 1, NASA, Washington, DC, SP 320, 1973, pp. 361–426.

[9]Lumley, J. L., "Computational Modeling of Turbulent Flows," *Advance in Applied Mechanics,* Vol. 18, 1978, pp. 123–176.

[10]Britter, R. E., Hunt, J. C. R., and Mumford, J. C., "The Distortion of Turbulence by a Circular Cylinder," *Journal of Fluid Mechanics,* Vol. 92, May 1979, pp. 269–301.

[11]Taulbee, D. B., Tran, L., and Dunn, M. G., "Stagnation Point and Surface Heat Transfer for a Turbine Stage: Prediction and Comparison with Data," *Proceedings of the 33rd International Gas Turbine Conference,* American Society of Mechanical Engineers, Paper 88-GT-30, June 1988.

Simple Expressions for Higher Vibration Modes of Uniform Euler Beams

John Dugundji*
Massachusetts Institute of Technology, Cambridge, Massachusetts

THE vibration modes and frequencies of uniform Euler beams for various boundary end conditions are traditionally expressed in terms of $\sin\beta_n x$, $\cos\beta_n x$, $\sinh\beta_n x$, and $\cosh\beta_n x$ functions (see, e.g., Refs. 1–3). For modes above the second, however, the numerical evaluation of these modes requires an increasingly large number of significant figures to be kept in order to distinguish small differences between $\sinh\beta_n x$ and $\cosh\beta_n x$. The present note, based on ideas presented in Ref. 3, gives simple expressions for arbitrarily high-order modes and fre- quencies of a uniform Euler beam. These expressions not only allow simple numerical calculation but also help to identify the physical nature of the modes.

Consider, for example, a free-free uniform Euler beam. The modes $\phi_n(x)$ and frequencies ω_n are traditionally expressed as

$$\phi_n(x) = \cosh\beta_n x + \cos\beta_n x - \alpha_n(\sinh\beta_n x + \sin\beta_n x) \quad (1)$$

$$\omega_n = \beta_n^2 \sqrt{EI/m\ell^4} \quad (2)$$

where β_n is the solution of the transcendental equation shown below, and α_n is related to β_n as indicated in Eq. (4).

$$\cos\beta_n = (1/\cosh\beta_n) \quad (3)$$

$$\alpha_n = \frac{\cosh\beta_n - \cos\beta_n}{\sinh\beta_n - \sin\beta_n} \quad (4)$$

Received Jan. 26, 1988.

*Professor, Department of Aeronautics and Astronautics. Member AIAA.